Results in Physics 8 (2018) 304–315

Contents lists available at ScienceDirect

Results in Physics

journal homepage: www.journals.elsevier.com/results-in-physics

Radiated chemical reaction impacts on natural convective MHD mass transfer flow induced by a vertical cone

P. Sambath [a], Bapuji Pullepu [a], T. Hussain [b,*], Sabir Ali Shehzad [c]

[a] Department of Mathematics, S R M University, Kattankulathur, Tamil Nadu 603203, India
[b] Department of Mathematics, University of Wah, WahCantt, Pakistan
[c] Department of Mathematics, Comsats Institute of Information Technology, Sahiwal 57000, Pakistan

ARTICLE INFO

Article history:
Received 27 July 2017
Received in revised form 9 November 2017
Accepted 2 December 2017
Available online 14 December 2017

Keywords:
Chemical reaction
Heat generation/absorption
MHD
Radiation
Vertical cone

ABSTRACT

The consequence of thermal radiation in laminar natural convective hydromagnetic flow of viscous incompressible fluid past a vertical cone with mass transfer under the influence of chemical reaction with heat source/sink is presented here. The surface of the cone is focused to a variable wall temperature (VWT) and wall concentration (VWC). The fluid considered here is a gray absorbing and emitting, but non-scattering medium. The boundary layer dimensionless equations governing the flow are solved by an implicit finite-difference scheme of Crank–Nicolson which has speedy convergence and stable. This method converts the dimensionless equations into a system of tri-diagonal equations and which are then solved by using well known Thomas algorithm. Numerical solutions are obtained for momentum, temperature, concentration, local and average shear stress, heat and mass transfer rates for various values of parameters Pr, Sc, λ, Δ, R_d are established with graphical representations. We observed that the liquid velocity decreased for higher values of Prandtl and Schmidt numbers. The temperature is boost up for decreasing values of Schimdt and Prandtl numbers. The enhancement in radiative parameter gives more heat to liquid due to which temperature is enhanced significantly.

Introduction

Numerical investigations of convection stimulated by the effect of buoyancy forces ensuing from thermal diffusion have always been significant attention to many researchers. Every natural convection process occurs in nature or in any scientific and engineering applications. Many researchers examined natural convection boundary layer flow of an electrically conducting fluid in the existence of MHD because of its relevances [1–5]. Inclusion of radiation field completely reliable with the fluid, called radiative hydrodynamics. Further, the radiative flows are commonly occurred in different engineering and ecological growth, e.g., heating and cooling compartments, relic energy burning, and desertion from vast open water tanks, planetary moves, and astral power tools [6–10].

Several authors developed similarity solutions for two-dimensional axi-symmetric problems of natural convection laminar flow over a vertical cone under steady state situation. General relations for similarity solutions on isothermal axi-symmetric and vertical cone problems have been established by Merk and Prins [11,12]. Hering and Grosh [13] showed that similarity solutions exist for steady free convection flow over vertical cone with variable surface temperature, and it varies as a power-law function of the distance from the apex along the cone ray. Numerical solutions of the transformed boundary layer equations were obtained for both an isothermal and linear surface temperature at the Prandtl number Pr = 0.7. Also noticed that the velocity and temperature in the case of an isothermal surface are higher by 22% than the corresponding values of these parameters in the case of linear surface temperature distribution.

Hering [14] extended the problem of Hering and Grosh [3] for low-Prandtl-number fluids and obtained numerical solutions for liquid metals. He concluded that the boundary layer thickness is greater for low-Prandtl-number fluids. Kafoussias [15] analyzed the effects of mass transfer on a free convective flow past a vertical cone surface embedded in an infinite, incompressible, and viscous fluid. Vajravelu and Nayfeh [16] methodically described the convection flow and heat transfer in a viscous heat generating fluid near a cone and wedge with variable surface temperature and internal heat generation or absorption. The governing flow and heat transfer equations are solved numerically by using a variable order, variable step size finite-difference method. Abd El-Naby et al. [17] obtained the solutions for the effects of radiation on an unsteady magneto hydrodynamic free convection flow past a

* Corresponding author.
E-mail address: zartotariq@yahoo.com (T. Hussain).

https://doi.org/10.1016/j.rinp.2017.12.005
2211-3797/© 2017 Published by Elsevier B.V.

Nomenclature

a, b	constants
C'	concentration in the fluid [mol m^{-3}]
C_P	specific heat [JKg^{-1}K^{-1}]
Gr_L	Grashof number (thermal)
g	gravitational force [ms^{-2}]
k_1	chemical reaction parameter (dimensional) [J]
L	referal length [m]
n	variationalpower law exponent in surface temperature
Nu_x	heat transfer rate (local)
Nu_X	local Nusselt number (non-dimensional)
Pr	Prandtl number
Q_0	heat generation and absorption coefficient (dimensional) [Wm^{-3}]
R_d	radiation (dimensionless)
Sc	Schmidt number
T	temperature (non-dimensional)
t	time (non-dimensional)
u	momentum over x direction (dimensional) [ms^{-1}]
v	momentum over y direction (dimensional)
x	spatial co-ordinate alongside the cone generator (dimensional) [m]
y	spatial co-ordinate perpendicular to cone generator (dimensional) [m]
B_0	magnetic field induction [*telsa*]
C'_∞	concentration far-away from cone surface
D	mass diffusivity [m^2 s^{-1}]
Gr_c	Grashof number (mass)
k	thermal conductivity [Wm^{-1} K^{-1}]
k^*	mean absorption coefficient [m^2]
m	variationalpower law exponent in surface concentration
N	ratio due to buoyancy force (non dimensional)
$\overline{Nu_L}$	heat transfer rate (average)
$\overline{Nu}$	average heat transfer rate (non-dimensional)
q_r	thermal radiation (dimensional)
R	local radius (dimensionless)
r	local radius of the cone [m]
T'	Temperature [K^0]
t'	Time [s]
U	momentum along X direction (non-dimensional)
V	momentum along Y direction (non-dimensional)
X	spatial co-ordinate alongside the cone generator (non-dimensional)
Y	spatial co-ordinate perpendicular to cone generator (non-dimensional)

Greek symbols

α	thermal diffusivity [m^2 s^{-1}]
β_c	coefficient of volumetric expansion due to concentration [^{0}k^{-1}]
λ	Parameter of chemical reaction (non-dimensional)
σ	electrical conductivity [sm^{-1}]
ϕ	cone apex half-angle [rad]
Δt	time step (non-dimensional)
ΔY	grid size (Ydirection) (non-dimensional)
ν	kinematic viscosity [m^2 s^{-1}]
τ_X	local shear stress (non-dimensional)
$\overline{\tau}$	average shear stress (non-dimensional)
β	volumetric thermal expansion [^{0}k^{-1}]
Δ	heat generation/absorption parameter (non-dimensional)
ρ	density [kg m^{-3}]
σ^*	Stefan-Boltzmann constant
$-\theta'(\infty, 0)$	local Nusselt number
ΔX	grid size (X direction) (non-dimensional)
μ	dynamic viscosity [kg m^{-1} s^{-1}]
τ_x	local shear stress
$\overline{\tau_L}$	average shear stress

Subscripts

w	wall condition
∞	free-stream condition

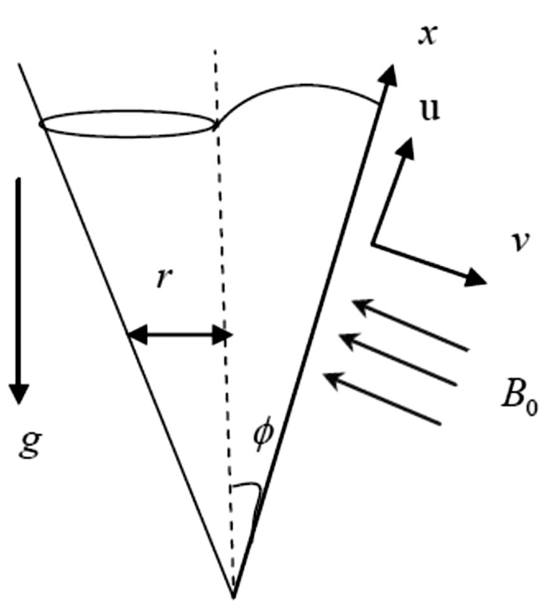

Fig. 1. Physical model and coordinate system.

Table 1
Comparison of steady-state local skin friction and local Nusselt number values at $X = 1.0$ with those of Chamkha [39] for full cone, for various values of Pr when $n = 0$, $M = 0, N = 0$ and $R_d = 0$.

	Local skin friction		Local Nusselt number	
	Chamkha [39]	Present values	Chamkha [39]	Present results
Pr	$f''(\infty, 0)$	$\tau_X/Gr_L^{\frac{3}{4}}$	$-\theta'(\infty, 0)$	$Nu_X/Gr_L^{\frac{1}{4}}$
0.001	1.5135	1.4149	0.0245	0.0294
0.01	1.3549	1.3356	0.0751	0.0797
0.1	1.0962	1.0911	0.2116	0.2115
1	0.7697	0.7688	0.5111	0.5125
10	0.4877	0.4856	1.0342	1.0356
100	0.2895	0.2879	1.9230	1.9316
1000	0.1661	0.1637	3.4700	3.5186

semi-infinite vertical porous plate in the presence of a transverse uniform magnetic field. Thandapani et al. [18] discussed the influence of a magnetic field and thermal radiation on natural convection over a vertical cone subjected to a variable surface temperature and they used Rosseland approximation to describe the radiative heat flux in the energy equation and the set of non-dimensional governing equations are solved by the finite-difference method. The unsteady mixed convection flow from a

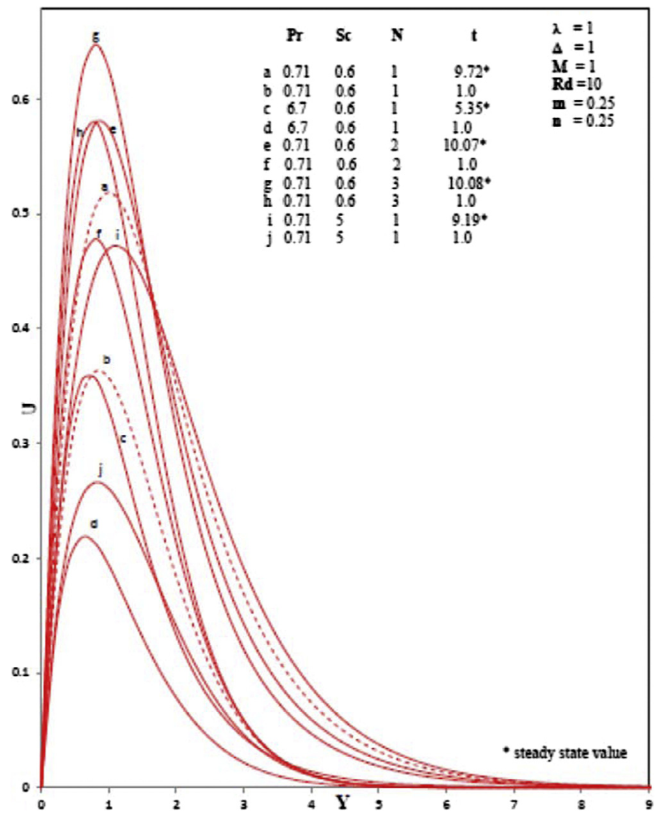

Fig. 2a. Transient velocity profiles at *X* = *1.0* for different values of *Pr*, *Sc* and *N*.

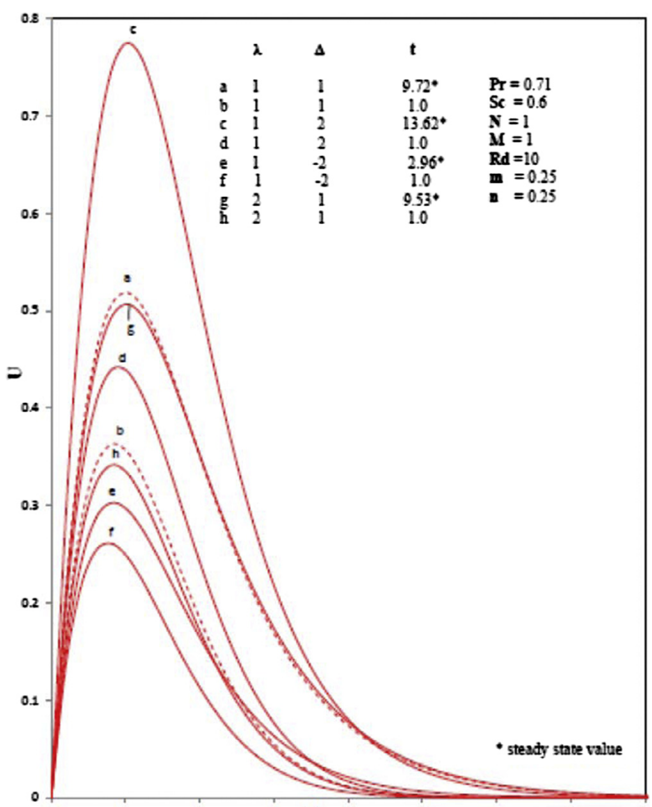

Fig. 2b. Transient velocity profiles at *X* = *1.0* for different values of *λ* and *Δ*.

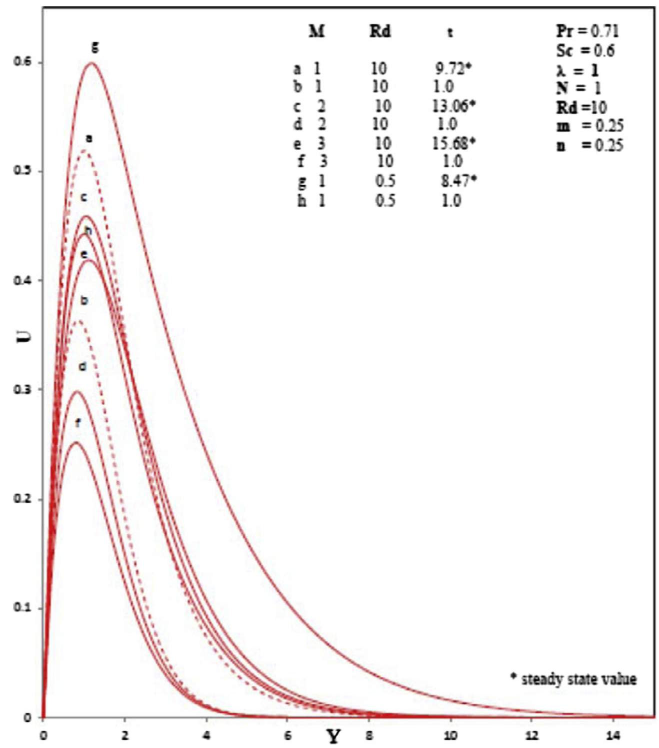

Fig. 2c. Transient velocity profiles at *X* = *1.0* for different values of *M* and *Rd*.

rotating vertical cone with a time dependent angular velocity under the influence of transverse magnetic field was investigated numerically by Takhar et al. [19]. Mahdy et al. [20,21] focused attention to the steady laminar free convection flow along a wavy cone and immersed in an electrically conducting fluid saturated porous medium in the presence of a transverse magnetic field and a vertical truncated cone with a Newtonian fluid having a viscosity proportional to an inverse linear function of temperature. Yih [22] presented numerical results for the radiation effects on natural convection over an isothermal truncated cone with the Rosseland diffusion approximation.

Suneetha et al. [23] attempted thermal radiation effects on MHD flow past an impulsively started vertical plate in the presence of heat source/sink by taking into account the heat due to viscous dissipation. The governing boundary layer equations of the flow field are solved by an implicit finite difference method of Crank-Nicholson type. EL-Kabeir and Abdou [24] studied the effects of chemical reaction, heat and mass transfer on MHD flow over a vertical isothermal cone surface in micro polar fluids with heat generation/absorption effects and obtained numerical solutions by using the fourth-order Runge-Kutta method with shooting technique.

Kishore et al. [25] presents a numerical study of thermal radiation effects on the transient hydro magnetic natural convection flow past a vertical plate embedded in a porous medium with mass diffusion and fluctuating temperature about time at the plate, by taking into account the heat due to viscous dissipation. The governing equations are solved by an implicit finite difference method of Crank–Nicolson type. Mohideen et al. [26] discussed the combined effects of thermal radiation and viscous dissipation on unsteady, laminar, free convective flow with heat and mass transfer over an incompressible viscous fluid past vertical cone with variable surface temperature and concentration in the presence of a transverse magnetic field applied normal to the surface. Also El- Kabeir et al. [27] discussed the linear transformation group approach to simulate the problem of heat and mass transfer in steady, two-dimensional, laminar, boundary-layer flow of a viscous, incompressible and electrically conducting fluid over a

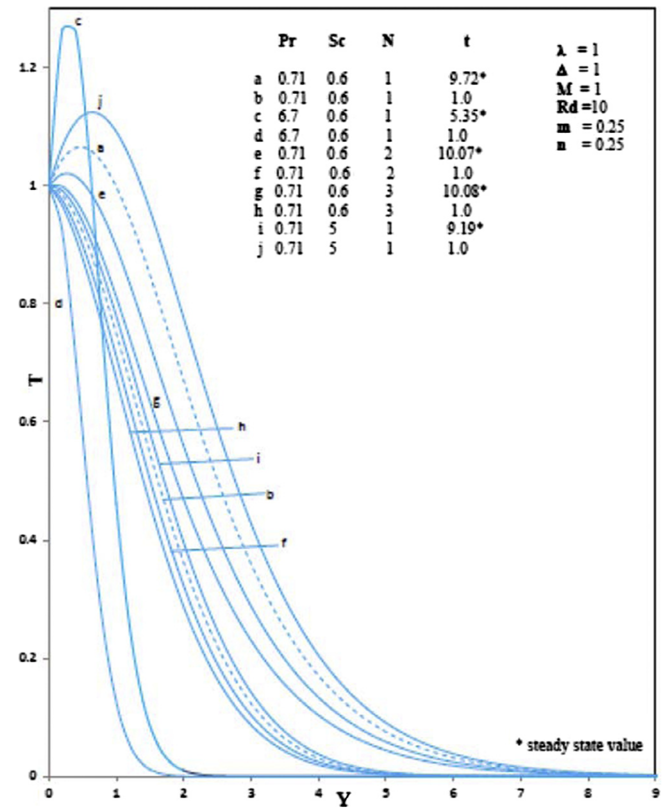

Fig. 3a. Transient temperature profiles at *X = 1.0* for different values of *Pr*, *Sc* and *N*.

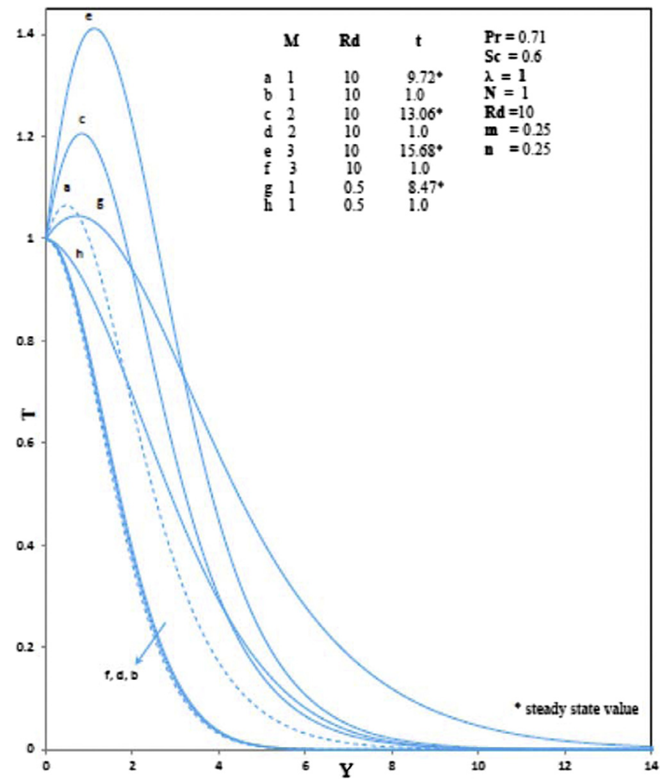

Fig. 3c. Transient temperature profiles at *X = 1.0* for different values of *M* and *Rd.*

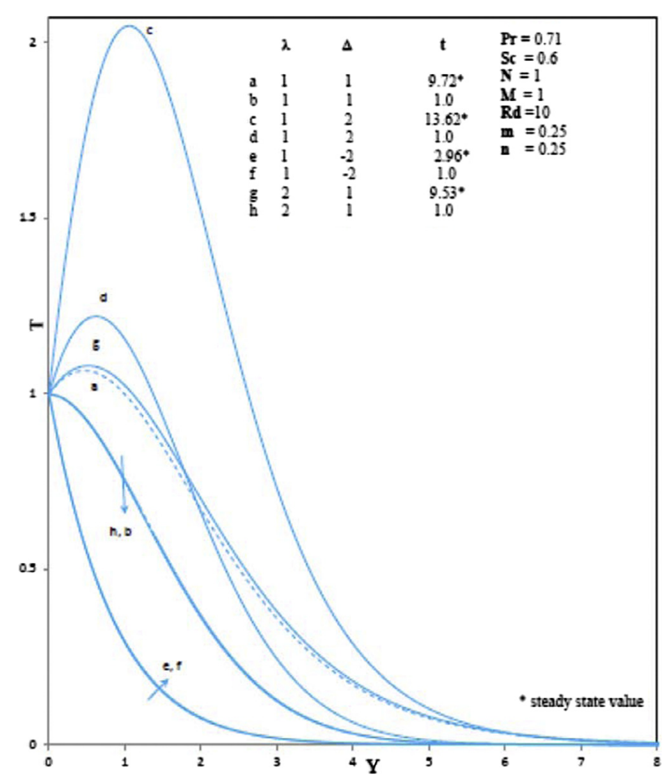

Fig. 3b. Transient temperature profiles at *X = 1.0* for different values of *λ* and *Δ.*

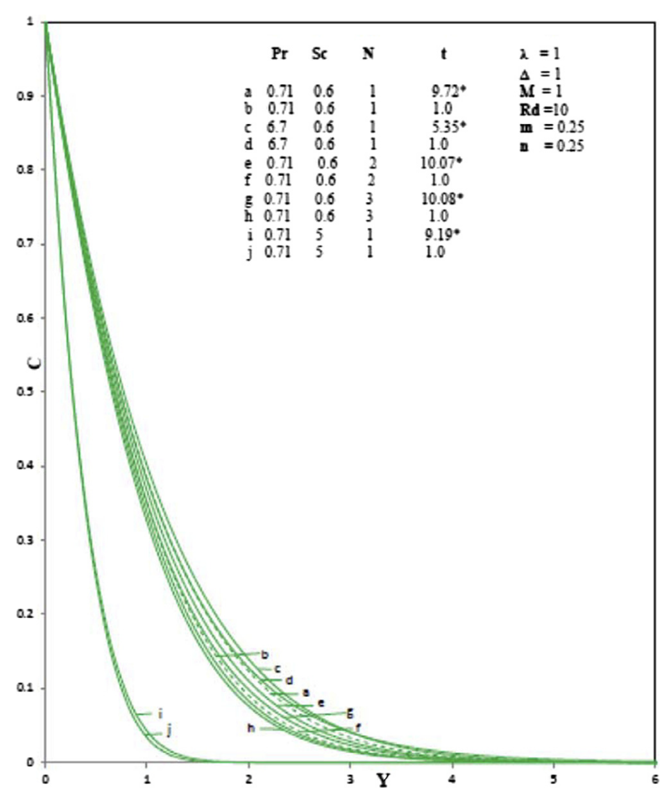

Fig. 4a. Transient concentration profiles at *X = 1.0* for different values of *Pr*, *Sc* and *N.*

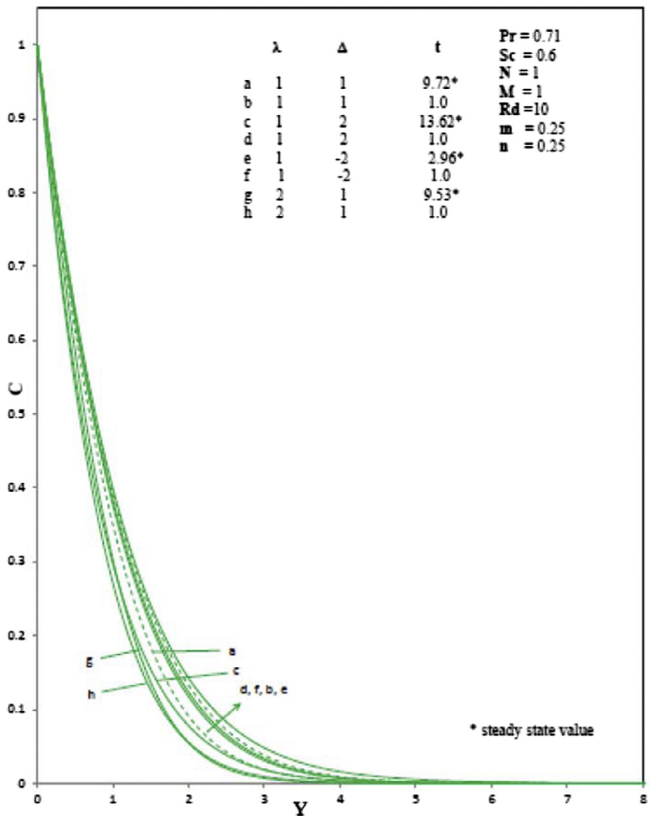

Fig. 4b. Transient concentration profiles at $X = 1.0$ for different values of λ and Δ.

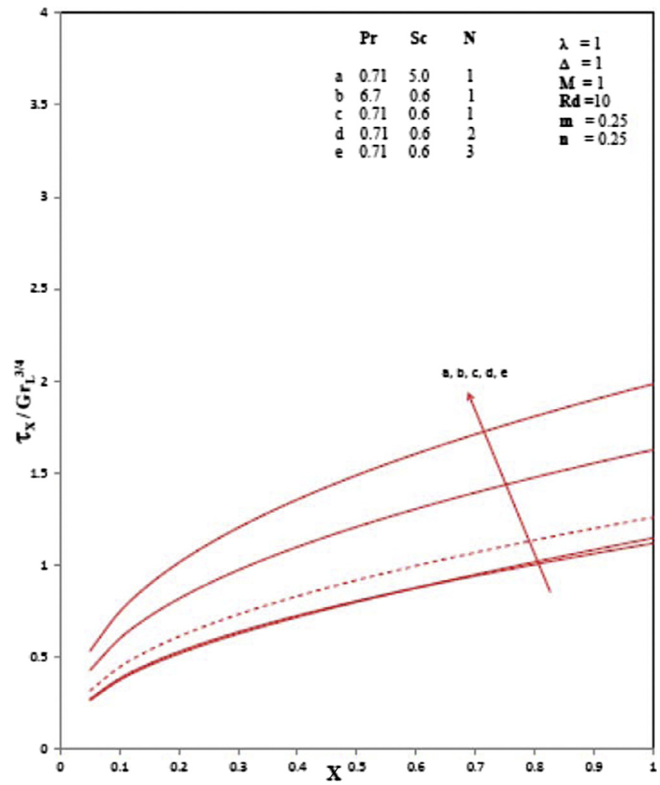

Fig. 5a. Local skin friction coefficients for different values of *Pr*, *Sc* and *N* in transient state.

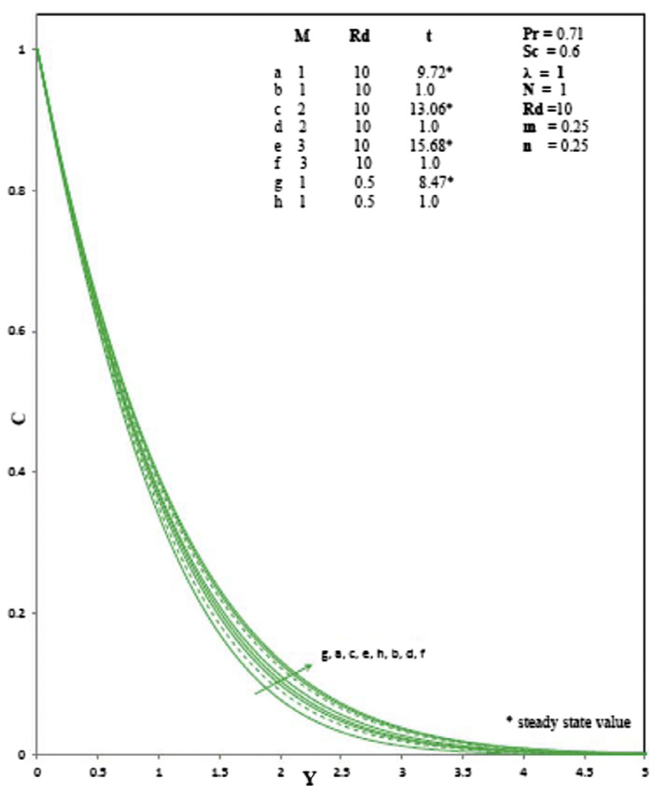

Fig. 4c. Transient concentration profiles at $X = 1.0$ for different values of *M* and *Rd*.

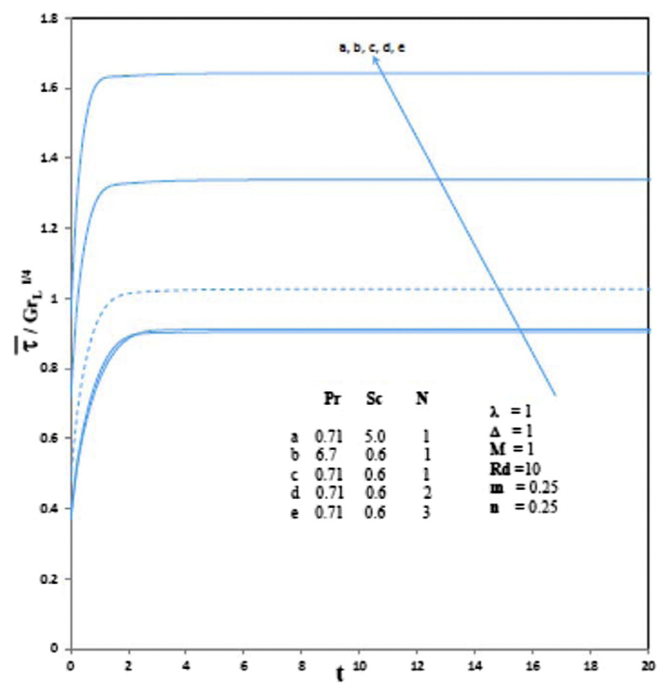

Fig. 5b. Average skin friction coefficients for different values of *Pr*, *Sc* and *N* in transient state.

vertical permeable cone surface saturated porous medium in the presence of a uniform transverse magnetic field and thermal radiation effects. Murti et al. [28] discussed the radiation and chemical reaction effects on heat and mass transfer in non-Darcy non Newtonian fluid over a vertical surface, the governing boundary layer equations and boundary conditions are simplified by using similarity transformations and are solved numerically by means of fourth-order Runge-Kutta method coupled with double-shooting technique.

El-Kabeir and El-Sayed [29] studied the problem of heat and mass transfer by free convection of a viscoelastic fluid past a vertical isothermal cone surface in the presence of transverse uniform magnetic field, and chemical reaction effect taking into account the effects of viscous dissipation, Joule heating and thermal radiation. The cone surface is maintained at constant temperature and constant species concentration. The governing partial differential equations are transferred into a system of ordinary differential equations, which are solved numerically using a fourth order Runge-Kutta scheme with the shooting method. Yih [30] discussed heat and mass transfer effects with UWT/UWC, UHF/UMF also the impacts of VWT/VWC and VHF/VMF. Bapuji et al. [31] studied the the effects of unsteady incompressible flow past a vertical cone with variable surface temperature varying as a power function of distance from the apex of the cone and magnetic field applied normal to the surface. The dimensionless coupled partial differential boundary layer equations are solved numerically using an efficient and unconditionally stable finite-difference scheme of the Crank-Nicolson type. The effects of radiation on free convection flow and mass transfer past a vertical isothermal cone surface with a chemical reaction in the presence of a magnetic field was investigated by Afify [32]. Transient flow through heat and mass transfer by rotating vertical cone with MHD effects was examined by Chamkha and Al-Mudhaf [33]. Muthucumaraswamy and Ganesan [34] considered radiation outcomes using infinite vertical plate. Chamka et al. [35] discussed radiation effects on mixed convection about a cone embedded in a porous medium filled with a nanofluid. Noghrehabadi et al. [36] discussed non-Darcy flow and natural convection over a vertical cone saturated with a nanofluid. Mohiddin et al. [37] discussed the boundary layer flow in a non-Darcian isotropic porous medium. Cheng [38] studied the heat transfer embedded in a tridisperse porous medium. Nayak et al. [39] executed the impact of chemical reaction in hydromagnetic non-Newtonian fluid flow saturated through porous space. The properties of time-dependent viscosity in third grade liquid has been addressed by Nayak et al. [40]. In another attempt, Nayak et al. [41] explored the analysis of wire coating for Oldroyd-8 constant liquid flow. The characteristics of heat ans mass transportation in time-dependent viscoelastic liquid flow over inclined porous plate has been reported by Nayak et al. [42]. Recently the following authors [43–53] discussed MHD flow with Casson fluid, chemically reacting fluid, radiation dufour effects, non darcy flow, visco elastic fluid flow over avertical cone, flat, vertical and wavy plates.

The influence of a magnetic field and thermal radiation on natural convection over a vertical cone subjected to a variable surface temperature and concentration has not received the attention of researchers. Hence an attempt is made to study the above said effects.

Mathematical analysis

Two-dimensional axi-symmetric, unsteady, laminar free convective MHD flow of a viscous incompressible electrically conducting fluid past a vertical cone is considered. In addition, we considered that the surface temperature and concentration are non uniform under the influence of chemical reaction, heat generation/absorption.

The effects of viscous dissipation in energy equation and pressure gradient along the boundary layer are negligible. There exists first order chemical reaction between the fluid and the species concentration, the joule heating of the fluid (magnetic dissipation) is neglected, the uniform transverse magnetic field is applied normal to the cone surface, thermal radiation is present in the form of a unidirectional flux q_r in the y direction, i.e., transverse to the cone surface. The radiative heat flux in the x direction is considered negligible in comparison with that in the y direction. The concentration C' of the diffusing species is assumed to be very small in comparison to the other chemical species far away from the surface of the cone C'_∞ hence the Soret and Dufour effects are neglected. The fluid considered is a gray absorbing/emitting, but non-scattering medium. Rosseland approximation is applied in the energy equation for the radiative heat flux, the cone surface and the surrounding fluid which is at rest are at the same temperature T'_∞ and concentration C'_∞. Then at time $t' > 0$, the temperature of the cone surface is suddenly raised to $T'_w(x) = T'_\infty + ax^n$ and the concentration near the cone surface is also raised to $C'_w(x) = C'_\infty + bx^m$ and both are maintained at the same level.

The coordinate system chosen (Fig. 1) is such that x measures the distance along the surface of the cone and y measures the distance perpendicular to it. The governing boundary layer equations of continuity, momentum, energy and concentration under Boussinesq approximation are as follows:

Equation of continuity

$$\frac{\partial}{\partial x}(ur) + \frac{\partial}{\partial y}(vr) = 0. \tag{1}$$

Equation of momentum

$$\frac{\partial u}{\partial t'} + u\frac{\partial u}{\partial x} + v\frac{\partial u}{\partial y} = g\beta(T' - T'_\infty)\cos\phi + \upsilon\frac{\partial^2 u}{\partial y^2} + g\beta_c(C' - C'_\infty) \times \cos\phi - \frac{\sigma B_0^2 u}{\rho}. \tag{2}$$

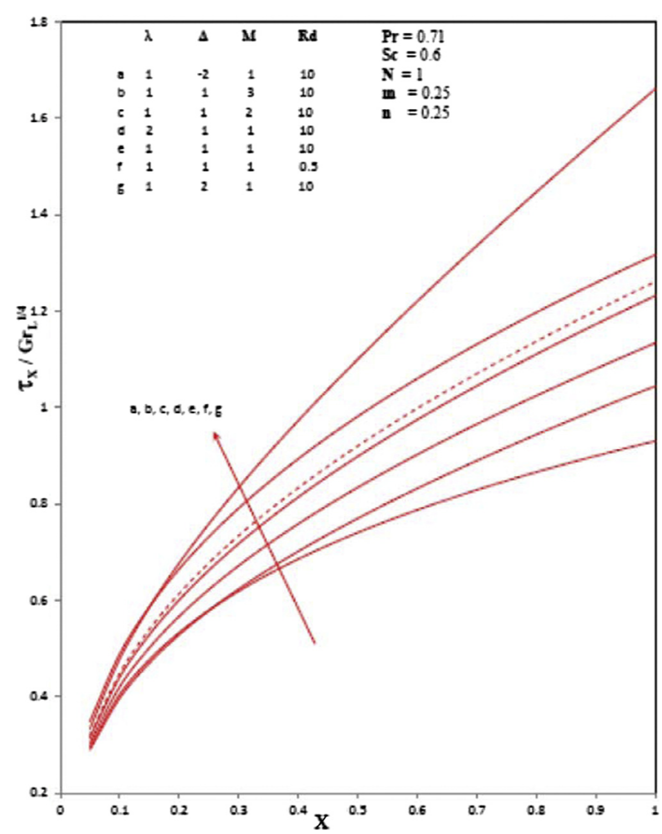

Fig. 5c. Local skin friction coefficients for different values of λ, Δ, M and Rd in transient state.

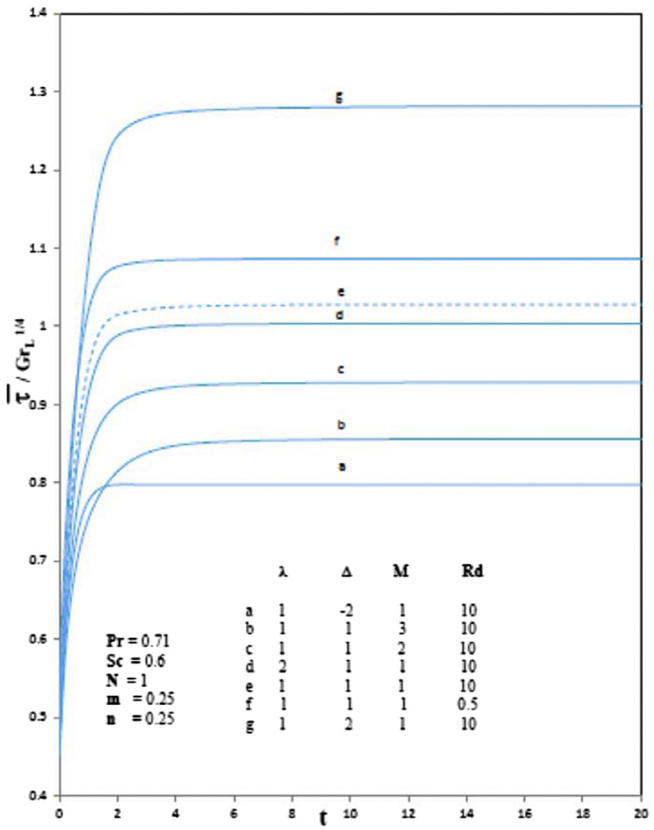

Fig. 5d. Average skin friction coefficients for different values of λ, Δ, M and Rd in transient state.

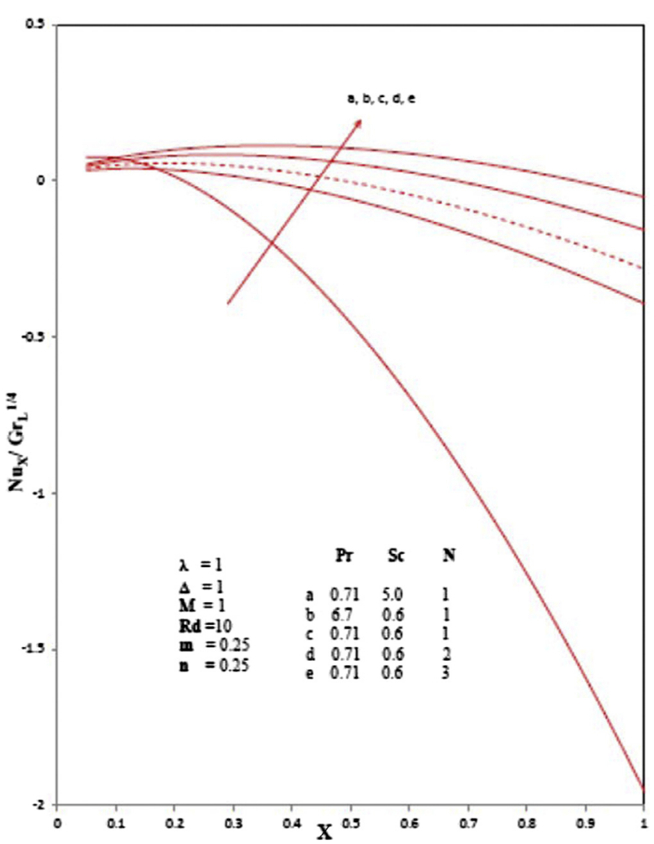

Fig. 6a. Local Nusselt number for different values of Pr, Sc and N in transient state.

Equation of energy

$$\frac{\partial T'}{\partial t'}+u\frac{\partial T'}{\partial x}+v\frac{\partial T'}{\partial y}=\alpha\frac{\partial^2 T'}{\partial y^2}+\frac{Q_o}{\rho c_p}(T'-T'_\infty). \tag{3}$$

Equation of concentration

$$\frac{\partial C'}{\partial t'}+u\frac{\partial C'}{\partial x}+v\frac{\partial C'}{\partial y}=D\frac{\partial^2 C'}{\partial y^2}-k_1(C'-C'_\infty). \tag{4}$$

The boundary conditions dimensional form are given below

$$\begin{aligned}&t'\leqslant 0: u=0,\ v=0, T'=T'_\infty, C'=C'_\infty \quad \text{for all } x \text{ and } y,\\ &t'>0: u=0,\ v=0, T'(x)=T'_\infty+ax^n, C'(x)=C'_\infty+bx^m \quad at\ \ y=0,\\ &u=0, T'=T'_\infty, C'=C'_\infty \quad at\ \ x=0,\\ &u\to 0, T'\to T'_\infty, C'\to C'_\infty \quad as\ \ y\to\infty.\end{aligned} \tag{5}$$

The expression $\frac{\partial q_r}{\partial y}$ in the energy equation is made simpler by employing the Rosseland approximation:

$$q_r=\frac{-4\sigma*}{3k*}\frac{\partial T'^4}{\partial y}. \tag{6}$$

It should be noted that we bound our investigation to optically thick fluids by using the Rosseland approximation. If the term $T'-T'_\infty$ inside the flow is adequately small, then the linear form of Eq. (6) can be obtained by escalating T'^4 by using the Taylor series expansion about T'_∞ by omitting upper-order terms.

We obtain

$$T'^4\approx T'^3_\infty T'-3T'^4_\infty. \tag{7}$$

Substituting Eqs. (6) and (7) in Eq. (3), we have

$$\frac{\partial T'}{\partial t'}+u\frac{\partial T'}{\partial x}+v\frac{\partial T'}{\partial y}=\alpha\frac{\partial^2 T'}{\partial y^2}+\frac{Q_o}{\rho c_p}(T'-T'_\infty)-\frac{1}{\rho c_p}\frac{16\sigma^* T'^3_\infty}{3k^*}\frac{\partial^2 T'}{\partial y^2}. \tag{8}$$

The local values of shear stress, heat transfer rate number and mass transfer rate are given by

$$\tau_x=\mu\left(\frac{\partial u}{\partial y}\right)_{y=0}, \tag{9}$$

$$Nu_x=\frac{-x\left(\frac{\partial T'}{\partial y}\right)_{y=0}}{T'_w-T'_\infty}, \tag{10}$$

$$Sh_x=\frac{-x\left(\frac{\partial C'}{\partial y}\right)_{y=0}}{C'_w-C'_\infty}. \tag{11}$$

The time dependence values of the above are given by

$$\overline{\tau_L}=\frac{2\mu}{L^2}\int_0^L x\left(\frac{\partial u}{\partial y}\right)_{y=0}dx. \tag{12}$$

The average heat transfer coefficient is given by

$$\overline{h}=\frac{-2k}{L^2}\int_0^L\frac{x\left(\frac{\partial T'}{\partial y}\right)_{y=0}}{T'_w-T'_\infty}dx, \tag{13}$$

$$\overline{N_{u_L}}=\frac{L\overline{h}}{k}=-\frac{2}{L}\int_0^L\frac{x\left(\frac{\partial T'}{\partial y}\right)_{y=0}}{T'_w-T'_\infty}dx, \tag{14}$$

$$\overline{S_{h_L}}=\frac{Lk_1}{D}=-\frac{2}{L}\int_0^L\frac{x\left(\frac{\partial C'}{\partial y}\right)_{y=0}}{C'_w-C'_\infty}dx. \tag{15}$$

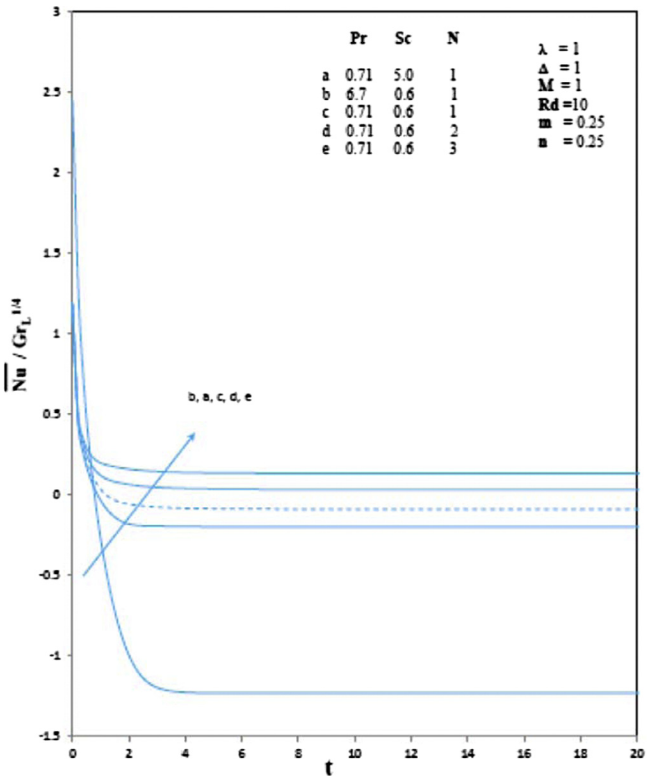

Fig. 6b. Average Nusselt number for different values of *Pr*, *Sc* and *N* in transient state.

Using the following non-dimensional quantities:

$$
\begin{aligned}
&X=\frac{x}{L}, Y=\frac{y}{L}(Gr_L)^{\frac{1}{4}},\ R=\frac{r}{L},\ \text{where } r=x\sin\phi,\\
&V=\frac{\upsilon L}{\upsilon}(Gr_L)^{\frac{-1}{4}},\ U=\frac{uL}{\upsilon}(Gr_L)^{\frac{-1}{2}},\ t=\frac{\upsilon t'}{L^2}(Gr_L)^{\frac{1}{2}},\\
&T=\frac{(T'-T'_\infty)}{(T'_w-T'_\infty)},\ Gr_L=\frac{g\beta(T'_w-T'_\infty)L^3\cos\phi}{\upsilon^2},\ \Pr=\frac{\upsilon}{\alpha},\\
&C=\frac{(C'-C'_\infty)}{(C'_w-C'_\infty)},\ Gr_C=\frac{g\beta_c(C'_w-C'_\infty)L^3\cos\phi}{\upsilon^2},\ Sc=\frac{\upsilon}{D},\\
&N=\frac{Gr_C}{Gr_L},\ \Delta=\frac{Q_oL^2}{C_p\mu}(Gr_L)^{\frac{-1}{2}},\ \lambda=\frac{k_1L^2}{\upsilon}(Gr_L)^{\frac{-1}{2}},\\
&M=\frac{\sigma B_0^2L^2}{\mu}Gr_L^{-1/2},\ R_d=\frac{K*K}{4\sigma*T'^3_\infty}.
\end{aligned}
\tag{16}
$$

The non-dimensional form of the governing equations are given below

Equation of continuity

$$\frac{\partial}{\partial X}(UR)+\frac{\partial}{\partial Y}(VR)=0. \tag{17}$$

Equation of momentum

$$\frac{\partial U}{\partial t}+U\frac{\partial U}{\partial X}+V\frac{\partial U}{\partial Y}=\frac{\partial^2 U}{\partial Y^2}+(T+NC)-MU. \tag{18}$$

Equation of energy

$$\frac{\partial T}{\partial t}+U\frac{\partial T}{\partial X}+V\frac{\partial T}{\partial Y}=\frac{1}{\Pr}\left(1+\frac{4}{3R_d}\right)\frac{\partial^2 T}{\partial Y^2}+\Delta T. \tag{19}$$

Equation of concentration

$$\frac{\partial C}{\partial t}+U\frac{\partial C}{\partial X}+V\frac{\partial C}{\partial Y}=\frac{1}{Sc}\frac{\partial^2 C}{\partial Y^2}-\lambda C. \tag{20}$$

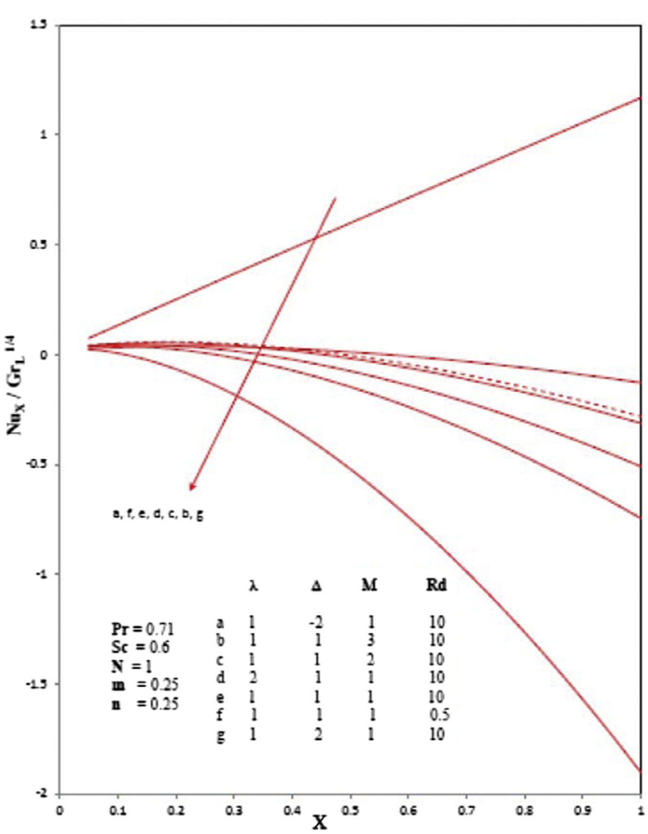

Fig. 6c. Local Nusselt number for different values of *λ*, Δ, *M* and *Rd* in transient state.

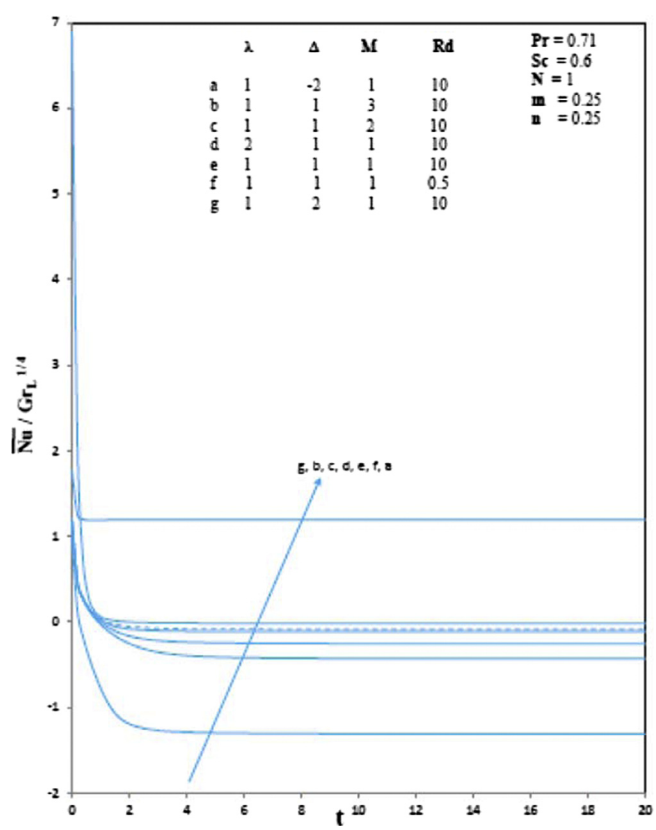

Fig. 6d. Average Nusselt number for different values of *λ*, Δ, *M* and *Rd* in transient state.

Initial and boundary conditions in non dimensional form are

$$\begin{aligned} &t \leqslant 0 : U = 0, \quad V = 0, \quad T = 0, \quad C = 0 \quad \text{for all} \quad X \text{ and } Y, \\ &t > 0 : U = 0, \quad V = 0, \quad T = X^n \text{ and } C = X^m \quad \text{at} \quad Y = 0, \\ &U = 0, \ T = 0, \ \ C = 0 \quad \text{at } X = 0, \\ &U \to 0, \ T \to 0, \ C \to 0 \quad \text{as } Y \to \infty \end{aligned} \tag{21}$$

shear stress, heat transfer rate and mass transfer rate in non-dimensional form given by

$$\tau_X = Gr_L^{\frac{3}{4}} \left(\frac{\partial U}{\partial Y} \right)_{Y=0}, \tag{22}$$

$$Nu_X = \frac{X}{T_{Y=0}} \left(\frac{-\partial T}{\partial Y} \right)_{Y=0} Gr_L^{\frac{1}{4}}, \tag{23}$$

$$Sh_X = \frac{X}{C_{Y=0}} \left(\frac{-\partial C}{\partial Y} \right)_{Y=0} Gr_L^{\frac{1}{4}}. \tag{24}$$

Dimensionless quantities for the average of skin-friction, Nusselt number and Sherwood number are

$$\overline{\tau} = 2Gr_L^{\frac{3}{4}} \int_0^1 X \left(\frac{\partial U}{\partial Y} \right)_{Y=0} dX, \tag{25}$$

$$\overline{Nu} = 2Gr_L^{\frac{1}{4}} \int_0^1 \frac{X}{T_Y = 0} \left(\frac{-\partial T}{\partial Y} \right)_{Y=0} dX, \tag{26}$$

$$\overline{Sh} = 2Gr_L^{\frac{1}{4}} \int_0^1 \frac{X}{C_Y = 0} \left(\frac{-\partial C}{\partial Y} \right)_{Y=0} dX. \tag{27}$$

Solution procedure

The transient, non-linear, coupled PDE's (17)–(20) along with (21) are worked out by using Crank-Nicholson method. After applying the method, the dimensionless equations converted to the system of tri-diagonal equations. We solve them by using well known Thomas algorithm by which we attain the desired solution with convergence of this algorithm occurring in a brief period of time and also it is unconditionally resistant to change. The integral area is treated as a square or with $X_{\max}$ (=1) and $Y_{\max}$ (=20) where $Y_{\max}$ corresponds to $Y = \infty$ which is located very well out side both the momentum and thermal layers are located out side of both the velocity and temperature periphery layers. The value for Y is taken to be 20 by analyzing in detail and considered in order to satisfy the ultimate and penultimate conditions of (20) and we observed that it is fulfilled with accuracy up to within the tolerance limit of 10^{-5}.

Results and discussion

In order to prove the accuracy of our numerical results, the present results for the steady-state flow at X = 1.0 are compared with available solutions from the open literature. The numerical values of the local skin friction τ_X and the local Nusselt number Nu_X for different values of the Prandtl number with M = 0, N = 0 and $R_d = 0$ are compared with the results of Chamkha [32] in Table 1.

Velocity, temperature, and concentration profiles at the upper edge of the cone i.e., at X = 1.0 for different values of Prandtl number Pr, Schmidt number *Sc*, the buoyancy ratio parameter *N* are shown through Figs. 2((a)–(c))–4((a)–(c)). It is found from Fig. 2a that the momentum boundary layer thickness increases for the fluids with Pr = 0.71 and decreases for Pr = 6.7. As the Schmidt number increases, the velocity and concentration decrease. This causes the concentration buoyancy effects to decrease yielding a reduction in the fluid velocity and velocity boundary layer. An increase in the buoyancy ratio parameter *N* leads to an increase in the velocity, i.e., as *N* increases, the combined buoyancy force also increases; therefore, the velocity increases near the surface of the cone as we move away from the surface of the cone, the temperature decreases for all the values of *N*.

Fig. 2b displays the effect of the chemical reaction parameter λ on the velocity profiles, the presence of the chemical reaction significantly affects the velocity profiles. As chemical reaction increases, the considerable reduction in the velocity profiles is observed. The boundary layer thickness decreases with an increase in the chemical reaction parameter λ and the presence of heat generation and absorption parameter Δ increases the velocity profiles. Fig. 2c depicts that the enhanced magnetic field, and radiation generates opposite force to the flow, is called Lorentz force. This force declines the velocity boundary layer thickness; it is also evident from the figure that the increase in thermal buoyancy parameter causes the increase in the velocity profiles of the fluid for both heat generation and absorption cases.

In Fig. 3a, we observe that the temperature decreases with increasing values of Prandtl number Pr. It is also observed that the thermal boundary layer thickness is maximum near the surface of the cone and decreases with increasing distances from the leading edge and finally approaches to zero. It is justified due to the fact that thermal conductivity of fluid decreases with increasing Prandtl number Pr and hence decreases the thermal boundary layer thickness and the temperature profiles. As the Schmidt number increases, the temperature increases. As we move away from the surface of the cone, the temperature decreases for all the values of the buoyancy ratio parameter *N*.

Fig. 3b depicts that the temperature increases for higher values of Δ and smaller values of Δ also the thermal boundary layer thickness increases. Fig. 3c shows that the increasing radiation parameter makes the fluid thick and ultimately causes the temperature

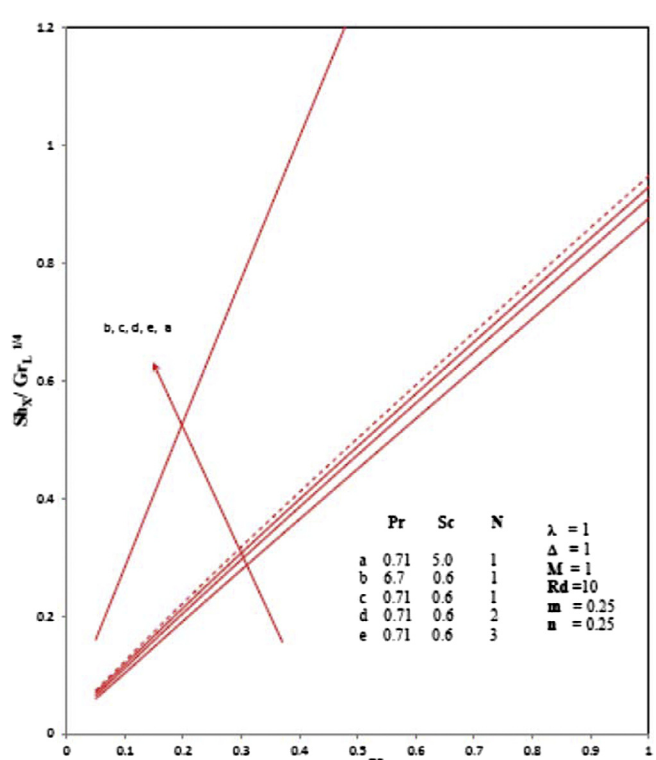

Fig. 7a. Local Sherwood number for different values of *Pr*, *Sc* and *N* in transient state.

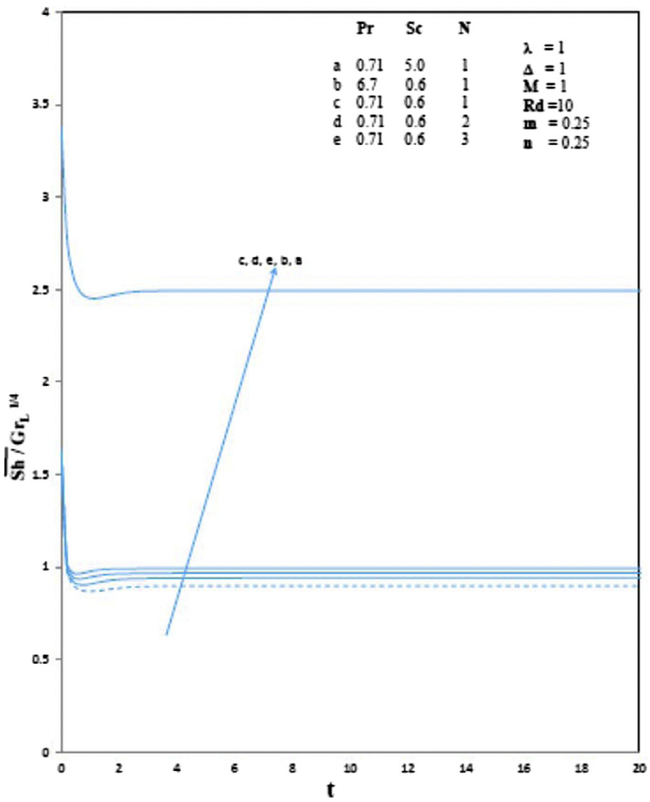

Fig. 7b. Average Sherwood number for different values of *Pr*, *Sc* and *N* in transient state.

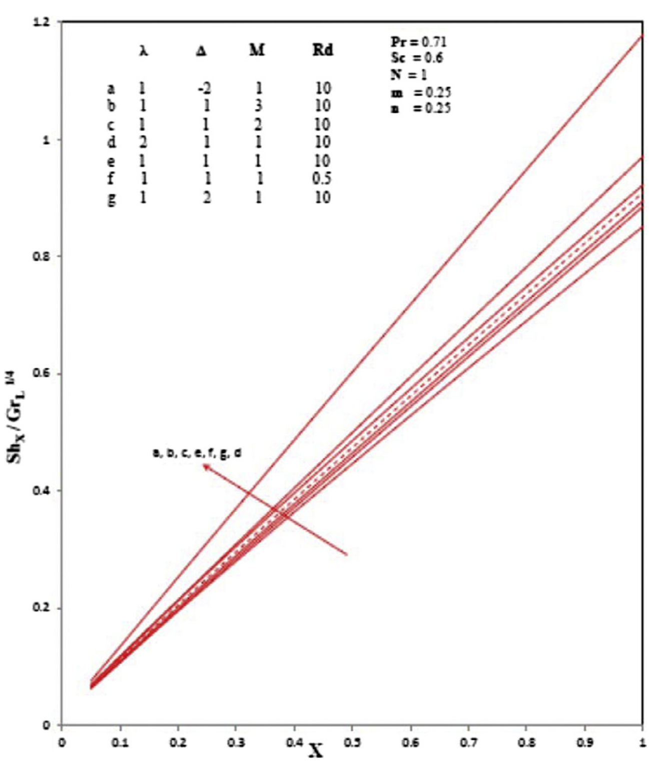

Fig. 7c. Local Sherwood number for different values of λ, Δ, *M* and *Rd* in transient state.

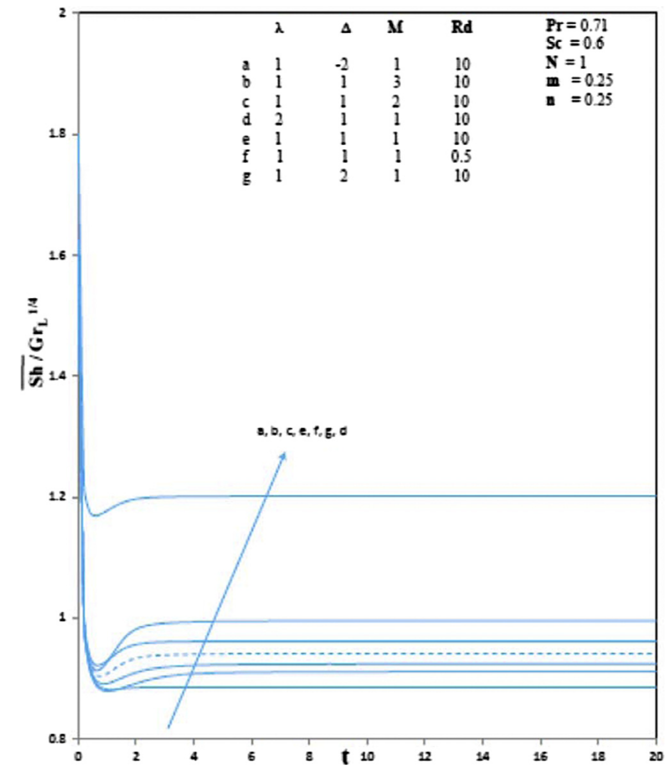

Fig. 7d. Average Sherwood number for different values of λ, Δ, *M* and *Rd* in transient state.

and the thermal boundary layer thickness to decrease hence we observe the decrease in temperature profiles for the presence of magnetic field and radiation effects.

Fig. 4a shows that the concentration buoyancy effects to decrease yielding a reduction in the fluid velocity and concentration. i.e. the concentration increases when Pr increases and decreases for increasing *Sc* and *N*. The velocity increases near the surface of the cone. Thus for higher values of buoyancy ratio parameter *N* the fluid cools rapidly and concentration field decreases with increasing value of buoyancy ratio parameter *N*. Fig. 4b shows the effect of the chemical reaction parameter λ and heat generation absorption parameter Δ on concentration profiles the presence of the chemical reaction, heat generation and absorption significantly affects the concentration profiles as λ and Δ increases, the concentration decreases. It is evident that the increase in Δ and λ alters the concentration boundary layer thickness but does not alter the momentum boundary layer.

Fig. 4c depicts the effect of magnetic field parameter and thermal radiation parameter on the concentration profiles The species concentration is highest at the cone surface and decreases to zero far away from the surface of the cone and the concentration boundary layer thickness decreases with a decrease in the magnetic field parameter *M* and radiation parameter *Rd*.

Figs. 5a and 5b illustrates the effects of Pr, *Sc* and *N* on the local and average skin friction. The local and average skin friction decreases for the increase in Pr and *Sc*. When Pr less than unity thermal diffusivity is will exceed momentum diffusivity, with increasing Pr values there is also a decrease in heat transfer rate whereas the skin friction is consistently boosted. Increasing Schmidt number which implies a decrease in mass diffusivity of the species is observed to suppress skin friction and heat transfer rates whereas it enhances the mass transfer rates. For $Sc = 0.6$ species diffusion rate exceeds the momentum diffusion rate and vice versa for $Sc = 2.66$.

For $Sc = 1$ both diffusion rates are the same and the momentum and concentration boundary layer thicknesses equal in the regime. The local and average skin friction increases for higher values of buoyancy ratio parameter N. Figs. 5c and 5d shows the effects of chemical reaction parameter λ heat generation and absorption parameter Δ, magnetic parameter M and thermal radiation parameter Rd on the local and average skin friction. Stronger thermal radiation accelerates the flow but reduces heat transfer rate hence the local and average skin friction got decreased due to the presence of magnetic field, and radiation where as it increases for the higher values of heat generation absorption parameter Δ chemical reaction parameter λ.

Figs. 6a and 6b shows the effects of Pr, Sc and N on the local and average Nusselt number. As Pr, Sc increases the local and average Nusselt number decreases and it increases as N increases. Since the positive buoyancy force acts like a favorable pressure gradient, the fluid is accelerated which results in thinner momentum and thermal boundary layers. Consequently, the Nusselt number and wall temperature increases with N.

Figs. 6c and 6d indicates the effects of chemical reaction parameter λ heat generation and absorption parameter Δ, magnetic parameter M and thermal radiation parameter Rd on the local and average Nusselt number. The local and average Nusselt number decreases for higher values Δ, λ, M and Rd.

Figs. 7a and 7b depicts the effects of Pr, Sc and N on the local and average Sherwood number. The local and average Sherwood number increases when Sc and N increase but decreases for higher values of Pr. Figs. 7c and 7d shows the effects of chemical reaction parameter λ heat generation and absorption parameter Δ, magnetic parameter M and thermal radiation parameter Rd on the local Sherwood number (mass transfer rate) and average Sherwood number, the local and average Sherwood number is considerably reduced in the presence of magnetic field and with increasing Rd values and Δ but the presence of chemical reaction increases the local and average Sherwood number.

Conclusions

The main findings are summarized as follows:

- The velocity increases for smaller values of Pr, Sc, M, λ and Rd but larger values of N, Δ lead to its decrement.
- The temperature increases for smaller values Pr, N, M, λ and Rd but it retard for larger values of Sc and Δ.
- Concentration increases with an increase in Pr, M and Rd and it retards for the increasing values of Sc, N, Δ and λ.
- An increase in the heat generation results in an increasing velocity and temperature within the boundary layer.
- The local and average skin-friction decrease with the increasing values of Pr, Sc, M, λ and Rd but increases for N and Δ.
- The local and average Nusselt number decreases with the increasing values of Pr, Sc, Δ, M, λ, M and Rd but increase for N.
- The local and average Sherwood number are weaker for larger values of Pr, Δ, M, and Rd but stronger in the case of higher Sc, N, λ.

References

[1] Sheikholeslami M, Rashidi MM, Ganji DD. Effect of non-uniform magnetic field on forced convection heat transfer of image-water nanofluid. Comput Methods Appl Mech Eng 2015;294:299–312.

[2] Hsiao K. Stagnation electrical MHD nanofluid mixed convection with slip boundary on a stretching sheet. Appl Thermal Eng 2016;98:850–61.

[3] Zhao J, Zheng L, Zhang X, Liu F. Convection heat and mass transfer of fractional MHD Maxwell fluid in a porous medium with Soret and Dufour effects. Int J Heat Mass Transf 2016;103:203–10.

[4] Hsiao K. Combined electrical MHD heat transfer thermal extrusion system using Maxwell fluid with radiative and viscous dissipation effects. Appl Thermal Eng 2017;112:1281–8.

[5] Sheikholeslami M, Shehzad SA. Magnetohydrodynamic nanofluid convection in a porous enclosure considering heat flux boundary condition. Int J Heat Mass Transf 2017;106:1261–9.

[6] Animasaun IL, Raju CSK, Sandeep N. Unequal diffusivities case of homogeneous-heterogeneous reactions within viscoelastic fluid flow in the presence of induced magnetic-field and nonlinear thermal radiation. Alex Eng J 2016;55:1595–606.

[7] Hayat T, Qayyum S, Shehzad SA, Alsaedi A. Simultaneous effects of heat generation/absorption and thermal radiation in magnetohydrodynamics (MHD) flow of Maxwell nanofluid towards a stretched surface. Results Phys 2017;7:562–73.

[8] Qayyum S, Khan MI, Hayat T, Alsaedi A. A framework for nonlinear thermal radiation and homogeneous-heterogeneous reactions flow based on silver-water and copper-water nanoparticles: A numerical model for probable error. Results Phys 2017;7:1907–14.

[9] Pal D, Mandal G. Thermal radiation and MHD effects on boundary layer flow of micropolar nanofluid past a stretching sheet with non-uniform heat source/sink. Int J Mech Sci 2017;126:308–18.

[10] Mahanthesh B, Gireesha BJ, Shashikumar NS, Shehzad SA. Marangoni convective MHD flow of SWCNT and MWCNT nanoliquids due to a disk with solar radiation and irregular heat source. Phys E: Low-dimensional Sys Nanostruc 2017;94:25–30.

[11] Merk HJ, Prins JA. Thermal convection laminar boundary layer I. Appl Sci Res 1953;4:11–24.

[12] Merk HJ, Prins JA. Thermal convection laminar boundary layer II. Appl Sci Res 1954;4:195–206.

[13] Hering RG, Grosh RJ. Laminar free convection from a non-isothermal cone. Int J Heat Mass Transf 1962;5:1059–68.

[14] Hering RG. Laminar free convection from a non-isothermal cone at low Prandtl number. Int J Heat Mass Transf 1965;8:1333–7.

[15] Kafoussias NG. Effects of mass transfer on Free convective flow past a vertical isothermal cone surface. Int J Eng Sci 1992;30:273–81.

[16] Vajravelu K, Nayfeh J. Hydro magnetic convection at a cone and a wedge. Int Commun. Heat Mass Transf 1992;19:701–10.

[17] El-Naby MA, Elbarbary MEE, Abdelazem Y. Nader, Finite difference solution of radiation effects on MHD unsteady free-convection flow over vertical plate with variable surface temperature. J Appl Math 2003;2:65–86.

[18] Thandapani E, Ragavan AR, Palani G. Finite-difference solution of unsteady natural convection flow past a non isothermal vertical cone under the influence of a magnetic field and thermal radiation. J Appl Mech Tech Phys 2012;53:408–21.

[19] Takhar HS, Chamkha AJ, Nath G. Unsteady mixed convection flow from a rotating vertical cone with a magnetic field. Heat Mass Transf 2003;39:297–304.

[20] Mahdy A, Chamkha AJ, Yousef B. Double-diffusive convection with variable viscosity from a vertical truncated cone in porous media in the presence of magnetic fieldn and radiation effects. Comput. Math. Appl. 2010;59:3867–78.

[21] Mahdy A, Mohamed RA, Hady FM. Influence of magnetic field on natural convection flow near a wavy cone in porous media. Latin Am Appl Res 2008;38:155–60.

[22] Yih KA. Radiation Effects on mixed convection over an isothermal cone in porous media. Heat Mass Transf 2001;37:53–7.

[23] Suneetha S, Reddy NB, Prasad RV. Radiation and mass transfer effects on MHD free convective dissipative fluid in the presence of heat source/sink. J Appl Fluid Mech 2011;4:107–13.

[24] El-Kabeir SMM, Abdou MMM. Chemical reaction, heat and mass transfer on MHD flow over a vertical isothermal cone surface in micropolar fluids with heat generation/absorption. Appl Math Sci 2007;1:1663–74.

[25] Kishore PM, Rajesh V, Vijayakumar SV. Viscoelastic buoyancy driven MHD free convective heat and mass transfer past avertical cone with thermal radiation and viscous dissipation effects. Int J Math Mech 2010;6:67–87.

[26] Mohiddin SG, Vijayakumar SV, Iyengar NCSN. Radiation and mass transfer effects on MHD free convective flow past a vertical cone with variable surface conditions in the presence of viscous dissipation. Int Electronic Eng Math Soc 2010;8:22–37.

[27] El-Kabeir SMM, El-Hakiem MA, Rashad AM. Group method analysis for the effect of radiation on MHD coupled heat and mass transfer natural convection flow water vapor over a vertical cone through porous medium. Int J Appl Math Mech 2007;3:35–53.

[28] Murti ASN, Kameswaran PK, Kantha TP. Radiation, chemical reaction, double dispersion effects on heat and mass transfer in non-Newtonian fluids. Int J Eng 2010;4:13–25.

[29] EL-Kabeir SMM, EL-Sayed EA. Effects of thermal radiation and viscous dissipation on MHD viscoelastic free convection past a vertical isothermal cone surface with chemical reaction. Int J Energy Tech 2012;4:1–7.

[30] Yih KA. Coupled heat and mass transfer by free convection over a truncated cone in porous media: VWT/VWC/ or VHF/VMF. Acta Mech 1999;137:83–97.

[31] Bapuji P, Chamkha AJ, Pop I. Unsteady laminar free convection flow past a non-isothermal vertical cone in the presence of magnetic field. Chem Eng Commun 2012;199:354–67.

[32] Afify AA. The effect of radiation on free convective flow and mass transfer past a vertical isothermal cone surface with chemical reaction in presence of transverse magnetic field. Can J Phys 2004;82:447–58.
[33] Chamkha AJ, Al-Mudhaf A. Unsteady heat and mass transfer from a rotating vertical cone with a magnetic field and heat generation or absorption effect. Int J Therm Sci 2005;44:267–76.
[34] Muthucumaraswamy R, Ganesan P. Radiation effects on flow past an impulsively started infinite vertical plate with variable temperature. Int J Appl Mech Eng 2003;8:125–9.
[35] Chamkha AJ, Abbasbandy S, Rashad AM, Vajravelu K. Radiation effects on mixed convection about a cone embedded in a porous medium filled with a nanofluid. Meccanica 2013;48:275–85.
[36] Noghrehabadi A, Behseresht A, Ghalambaz M. Natural-convection flow of nanofluids over vertical cone, embedded in non-Darcy porous media. J Thermophys Heat Transf 2013;27:334–41.
[37] Mohiddin SG, Beg OA, Varma SVK. Numerical study of free convective MHD flow past a vertical cone in non-Darcian porous media. Theor Appl Mech 2014;4:119–40.
[38] Cheng C. Natural convection heat transfer about a vertical cone embedded in a tridisperseporousmedium. Trans Porous Med 2015;107:765–79.
[39] Nayak MK, Dash GC, Singh LP. Effect of chemical reaction on MHD flow of a viscoelastic fluid through porous medium. J Appl Anal Comput 2014;4:367–81.
[40] Nayak MK, Dash GC, Singh LP. Steady MHD flow and heat transfer of a third grade fluid in wire coating analysis with temperature dependent viscosity. Int J Heat Mass Transf 2014;79:1087–95.
[41] Nayaka MK, Dash GC. A numerical study on wire coating analysis in MHD flow of an Oldroyd 8-constant fluid. Model Measure Control B 2015;84:125–39.
[42] Nayak MK, Dash GC, Singh LP. Unsteady radiative MHD free convective flow and mass transfer of a viscoelastic fluid past an inclined porous plate. Arab J Sci Eng 2015;40:3029–39.
[43] Chamkha AJ. Coupled heat and mass transfer by natural convection about a truncated cone in the presence of magnetic field and radiation effects. Numer Heat Transf 2001;39:511–30.
[44] Benazir J, Sivaraj R, Makinde OD. Unsteady MHD Casson fluid flow over a vertical cone and flat plate with non-uniform heat source/sink. Int Eng Res Africa 2015;21:69–83.
[45] Kumar BR, Sivaraj R, Benazir AJ. Chemically reacting MHD free convective flow over a vertical cone with variable electric conductivity. Int J Pure Appl Math 2015;101:821–8.
[46] Prakash J, Kumar BR, Sivaraj R. Radiation and Dufour effects on unsteady MHD mixed convective flow in an accelerated vertical wavy plate with varying temperature and mass diffusion. Walailak J Sci Tech 2014;11:939–54.
[47] Kumar BR, Sivaraj R. MHD viscoelastic fluid non-Darcy flow over a vertical cone and a flat plate. Int Commun Heat Mass Transf 2013;40:1–6.
[48] Kumar BR, Sivaraj R. Heat and mass transfer in MHD viscoelastic fluid flow over a vertical cone and flat plate with variable viscosity. Int J Heat Mass Transf 2013;56:370–9.
[49] Nayak MK. Chemical reaction effect on MHD viscoelastic fluid over a stretching sheet through porous medium. Meccanica 2016;51:1699–711.
[50] Nayak MK, Akbar NS, Pandey VS, Khan ZH, Tripathi D. 3D free convective MHD flow of nanofluid over permeable linear stretching sheet with thermal radiation. Powder Tech 2017;315:205–15.
[51] Nayak MK, Akbar NS, Tripathi D, Khan ZH, Pandey VS. MHD 3D free convective flow of nanofluid over an exponentially stretching sheet with chemical reaction. Adv Powder Tech 2017;28:2159–66.
[52] Nayak MK, Akbar NS, Tripathi D, Pandey VS. Three dimensional MHD flow of nanofluid over an exponential porous stretching sheet with convective boundary conditions. Thermal Sci Eng Prog 2017;3:133–40.
[53] Nayak MK. MHD 3D flow and heat transfer analysis of nanofluid by shrinking surface inspired by thermal radiation and viscous dissipation. Int J Mech Sci 2017;124:185–93.